

## Supporting Information

### Insights into the folding of disulfide-rich $\mu$ -conotoxins

Ajay Abisheck Paul George<sup>a</sup>, Pascal Heimer<sup>a</sup>, Astrid Maaß<sup>b</sup>, Jan Hamaekers<sup>b</sup>, Martin Hofmann-Apitius<sup>c,d</sup>, Arijit Biswas<sup>e</sup>, and Diana Imhof<sup>a\*</sup>

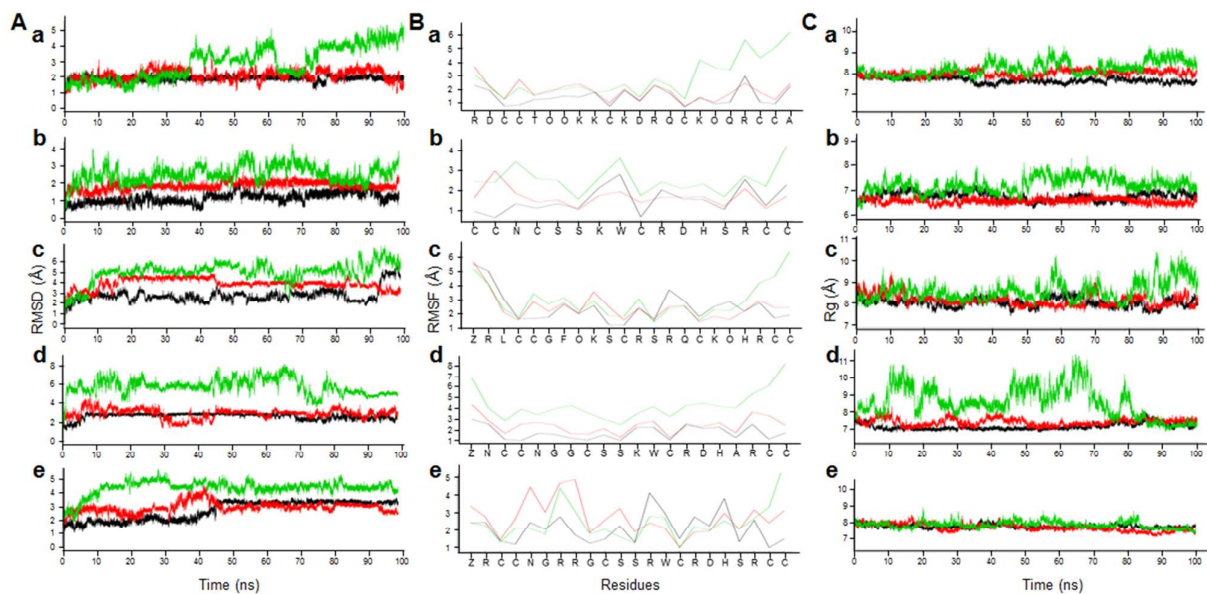
#### Table of contents

##### Supporting Figures

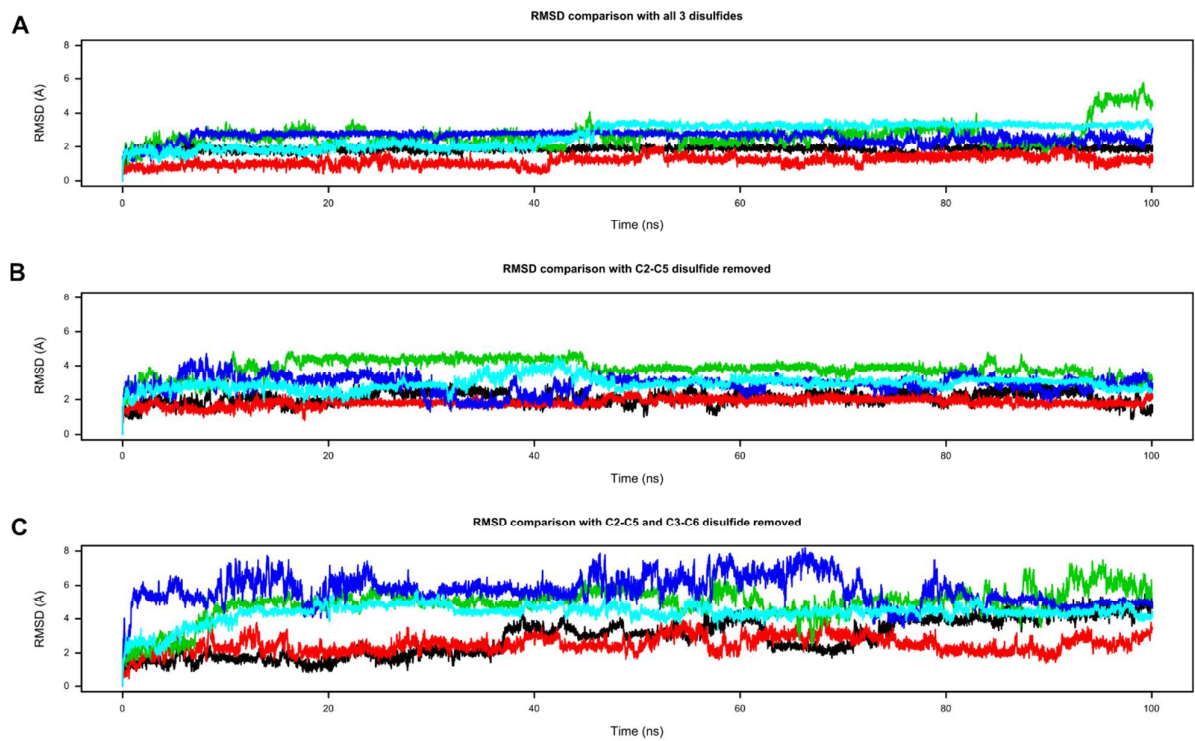
S1. RMSD, RMSF, and Rg of the five $\mu$ -conotoxins	2
S2. Backbone stability of the five $\mu$ -conotoxins with 3, 2, and 1 disulfide-bridge	3
S3. Backbone conformation of $\mu$ -GIIIA and $\mu$ -SmIIIA, helix formation	4
S4. Backbone conformation of $\mu$ -PIIIA, loss of helix by disulfide-bond removal	5

##### Supporting Tables

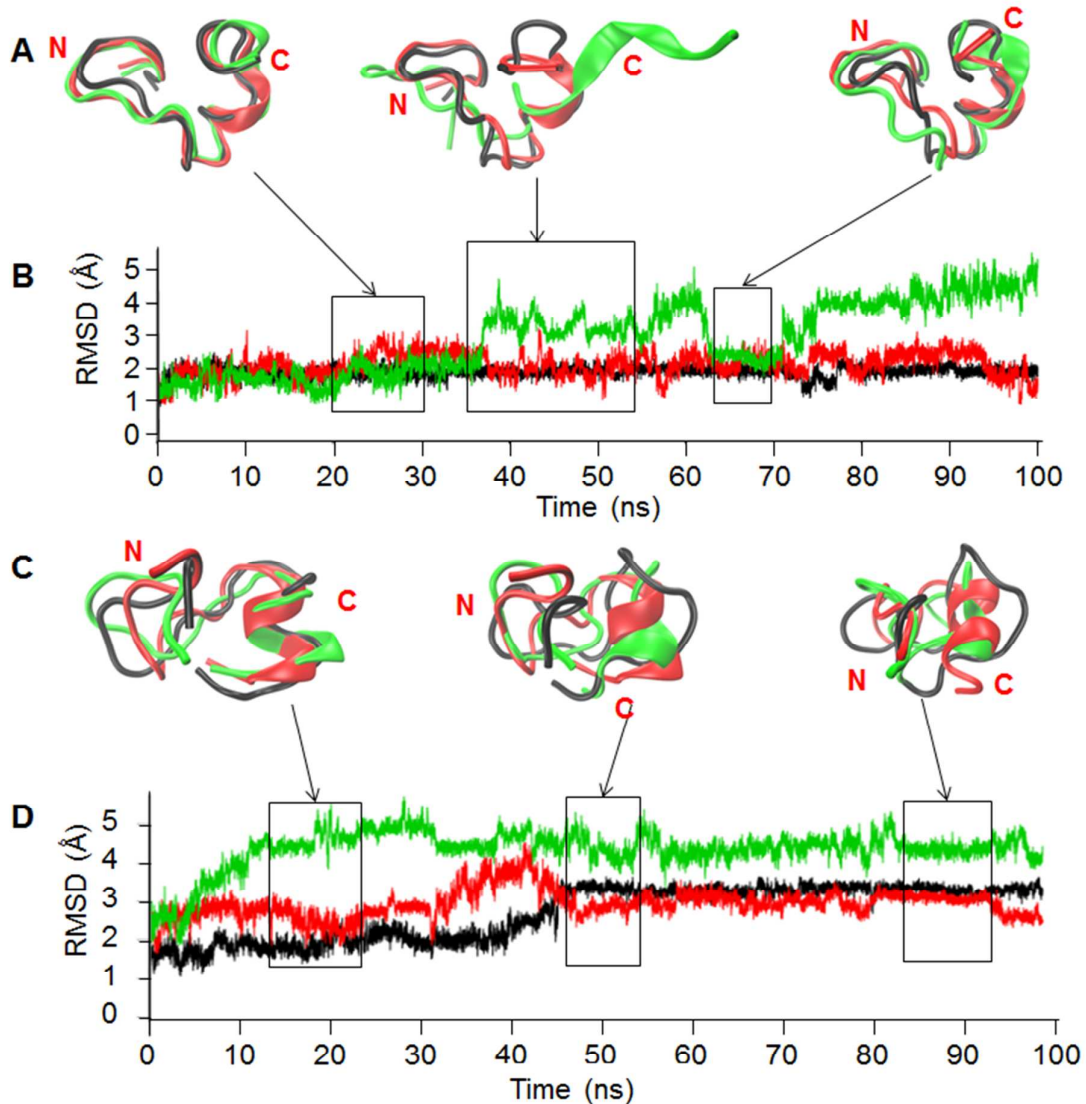
S1. Comparison of disulfide loop length of the five $\mu$ -conotoxins	6
S2. Assessment of stability using RMSD and Rg for 100 ns MD simulation	7
S3. Impact of the C2-C5 and C3-C6 disulfide bridge on the backbone RMSF and the functionally stable residues	8



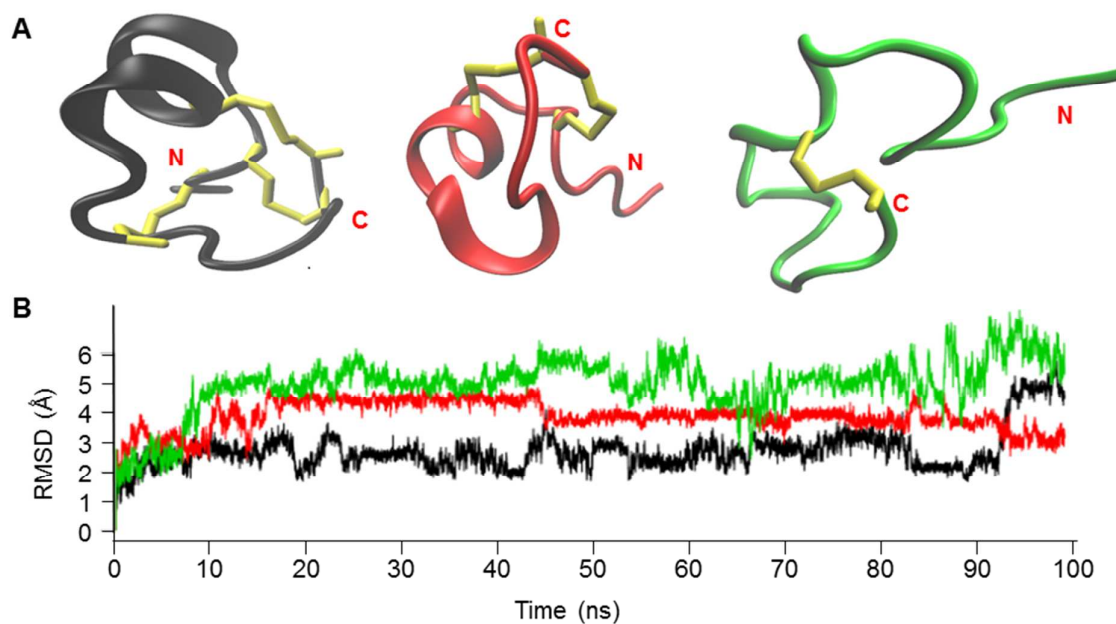
**Supporting Figure S1.** Determination of peptide stability with RMSD (A), RMSF (B) and radius of gyration (C). All plots of the five  $\mu$ -conotoxins are in alphabetic order: (a) GIIIA, (b) KIIA, (c) PIIA, (d) SIIA, and (e) SmIIA. In general, the peptide native fold is represented in black, the peptide with one bridge opened is shown in red, and the peptide with two open bonds is in green. Values are given in Table S2.



**Supporting Figure S2.** Backbone stability of the five  $\mu$ -conotoxins (black: GIIIA, red: KIIIA, green: PIIIA, blue: SIIIA, cyan: SmIIIA) in the native state (A), with disulfide bridge C2–C5 removed (B), and with two disulfide bridges C2–C5, C3–C6 removed (C). In the case of  $\mu$ -KIIIA the C2–C4 and C3–C6 bonds were opened in the native fold.



**Supporting Figure S3.** Backbone stability of  $\mu$ -GIIIA and  $\mu$ -SmIIIA. In general, the peptide native fold is represented in black, the peptide with one bridge opened is shown in red, and the peptide with two open bonds is in green. (A)  $\mu$ -GIIIA average structures obtained and superimposed from 20 ns – 30 ns, 35 ns – 55 ns, and 65 ns – 70 ns. (B) RMSD for a simulation time of 100 ns of the respective peptide. In both cases, when compared with the native structure, the structure containing two disulfide bonds displays consistent structural stability. (C)  $\mu$ -SmIIIA average structures obtained and superimposed from 15 ns – 25 ns, 45 ns – 55 ns, and 85 ns – 95 ns. (D) RMSD for a simulation time of 100 ns of the respective peptide. In contrast to the native structure the appearance of helices in the structures after disulfide bonds removed is noteworthy resulting in comparable stability. Helix formation in  $\mu$ -GIIIA occurs between residues D12 and Q18. In  $\mu$ -SmIIIA helix formation is between the residues W14 and R20.



**Supporting Figure S4.** (A) Representation of  $\mu$ -P11IA for native (black), one disulfide bridge (C2-C5, red) and two disulfide bridges (C2-C5, C3-C6, green) removed. (B) Backbone RMSD for the three peptides for 100 ns.

**Supporting Table S1.** Comparison of disulfide loop length of the five  $\mu$ -conotoxins. For the  $\mu$ -conotoxins GIIIA, PIIIA, SIIIA and SmIIIA the values corresponding to disulfide loops 1, 2 and 3 is the number of residues present between the C1-C4, C2-C5 and C3-C6 disulfide bridges, respectively. For  $\mu$ -KIIIA, the disulfide loops 1, 2 and 3 correspond to the number of residues occurring between the disulfide bridges C1-C5, C2-C4 and C3-C6.

$\mu$ -Conotoxin	Disulfide loop 1	Disulfide loop 2	Disulfide loop 3
GIIIA	11	15	10
KIIIA	15	6	11
PIIIA	11	15	10
SIIIA	9	14	11
SmIIIA	11	16	11

**Supporting Table S2.** Assessment of stability using RMSD and radius of gyration for 100 ns MD simulation.

$\mu$ -Conotoxin	No. of disulfide bonds	C $\alpha$ RMSD (Å)	Radius of gyration (Å)
GIIIA	3	1.8	7.6
	2	2.1	8.0
	1	2.8	8.2
KIIIA	3	1.1	6.7
	2	1.8	6.5
	1	2.5	7.1
PIIIA	3	2.3	8.0
	2	3.8	8.1
	1	4.9	8.5
SIIIA	3	2.6	7.0
	2	2.8	7.35
	1	5.7	8.5
SmIIIA	3	2.7	7.7
	2	2.9	7.6
	1	4.3	7.8

**Supporting Table S3.** Impact of the C2-C5 and C3-C6 disulfide bridge removal on the backbone and the functionally stable residues. Column 2 lists residues in each  $\mu$ -conotoxin that are significant for binding affinity as reported by Akondi *et al.*<sup>6</sup> Column 3 gives the difference (in brackets) in residue fluctuation between the native form and the C2-C5 disulfide bond removed form of the five  $\mu$ -conotoxins. Column 4 reports the difference in residue fluctuation between the native form and two-disulfide-bond-removed conformations. The RMSF values are used as basis for determining increase or decrease of flexibility. A difference of close to 2 Å between RMSF values is considered significant and is marked in bold. \*In the case of  $\mu$ -KIIIA the C2-C4 disulfide bridge is removed. \*\*Besides the general statement for the conserved basic residue between C3 and C4 essential for biological activity of  $\mu$ -conotoxins, no order of basic residues is described so far.

$\mu$ -Conotoxin	Functional basic residues in order of significance on biological activity against Na <sub>v</sub> 1.4	Comparison of flexibility on removal of the C2-C5* disulfide bridge (in Å)	Comparison of flexibility on removal of the C2-C5* and C3-C6 disulfide bridge (in Å)
GIIIA	R13 > R19 > R1, K8, K11, K16 > K9 <sup>1,2</sup>	R13 (0), R19 (0.5), R1 (0.7), K8(0.9), K11(0.1), K16 (0) K9 (0.1)	R13 (0.5), <b>R19 (2.6)</b> , R1 (0.8), K8(0.7), K11(0.5), <b>K16 (2.8)</b> , K9 (0)
KIIIA	H12 > R14 > K7 > R10 <sup>3,4</sup>	H12 (0.2), R14 (0.5), K7 (0.4), R10 (0.3)	H12 (0.8), R14 (0.9), K7 (0.5), R10 (0.4)
PIIIA	R14 > K17 > R12, R20, R2, K9 <sup>5</sup>	R14 (1.3), K17 (0.7), R12 (0), R20 (0.2), R2 (0.9), K9 (1)	R14 (1.4), K17 (0.2), R12 (0.6), R20 (1.4), R2 (0.9), K9 (0.3)
SIIIA	R14 > K11, H16, R18**	R14 (0.4), K11 (0.3), H16 (0.4), R18 (1.1)	<b>R14 (1.7)</b> , K11 (1.2), <b>H16 (1.9)</b> , <b>R18 (2.8)</b>
SmIIIA	R13 > R7, R8, R16, R20**	R13 (1.4), <b>R7 (1.6)</b> , R8 (1.2), R16 (0.6), R20 (0.1)	<b>R13 (1.8)</b> , <b>R7 (1.9)</b> , <b>R8 (2.2Å)</b> , R16 (0.6), R20 (0.1)



## References

- (1) Choudhary, G.; Aliste, M. P.; Tieleman, D. P.; French, R. J.; Dudley Jr., S. C. Docking of  $\mu$ -Conotoxin GIIIA in the Sodium Channel Outer Vestibule. *Channels* **2007**, *1* (5), 344–352.
- (2) Sato, K.; Ishida, Y.; Wakamatsu, K.; KJato, R.; Honda, H.; Ohizumi, Y.; Nakamura, H.; Ohya, M.; Lancelin, J.-M.; Kohda, D.; et al. Active Site of M-Conotoxin GIIIA, a Peptide Blocker of Muscle Sodium Channels. *J. Biol. Chem.* **1991**, *266* (26), 16989–16991.
- (3) McArthur, J. R.; Singh, G.; McMaster, D.; Winkfein, R.; Tieleman, D. P.; French, R. J. Interactions of Key Charged Residues Contributing to Selective Block of Neuronal Sodium Channels by  $\mu$ -Conotoxin KIIIA. *Mol. Pharmacol.* **2011**, *80* (4), 573–584.
- (4) Mahdavi, S.; Kuyucak, S. Systematic Study of Binding of M-Conotoxins to the Sodium Channel Nav1.4. *Toxins (Basel)*. **2014**, *6* (12), 3454–3470.
- (5) McArthur, J. R.; Singh, G.; O'Mara, M. L.; McMaster, D.; Ostroumov, V.; Tieleman, D. P.; French, R. J. Orientation of  $\mu$ -Conotoxin PIIIA in a Sodium Channel Vestibule, Based on Voltage Dependence of Its Binding. *Mol. Pharmacol.* **2011**, *80* (2), 219–227.
- (6) Akondi, K. B.; Muttenthaler, M.; Kaas, Q.; Craik, D. J.; Lewis, R. J.; Alewood, P. F. Discovery , Synthesis, and Structure – Activity Relationships of Conotoxins. *Chem. Rev.* **2013**, *114* (11), 5815-5847.